Research Article | Vol. 10, No. 9 | 1 Sep 2019 | BIOMEDICAL OPTICS EXPRESS 4381
Biomedical Optics EXPRESS

Green fluorescent protein emission obscures metabolic fluorescent lifetime imaging of NAD(P)H

ELISA M. YORK,[1,2] NICHOLAS L. WEILINGER,[1] JEFFREY M. LEDUE,[1] AND BRIAN A. MACVICAR[1,3]

[1]*Department of Psychiatry, Djavad Mowafaghian Centre for Brain Health, University of British Columbia, British Columbia, Canada*
[2]*elisa.york@alumni.ubc.ca*
[3]*bmacvicar@brain.ubc.ca*

Abstract: Autofluorescence of endogenous molecules can provide valuable insights in both basic research and clinical applications. One such technique is fluorescence lifetime imaging (FLIM) of NAD(P)H, which serves as a correlate of glycolysis and electron transport chain rates in metabolically active tissue. A powerful advantage of NAD(P)H-FLIM is the ability to measure cell-specific metabolism within heterogeneous tissues. Cell-type specific identification is most commonly achieved with directed green fluorescent protein (GFP) expression. However, we demonstrate that NAD(P)H-FLIM should not be analyzed in GFP-expressing cells, as GFP molecules themselves emit photons in the blue spectrum with short fluorescence lifetimes when imaged using two-photon excitation at 750 nm. This is substantially different from the reported GFP emission wavelength and lifetime after two-photon excitation at 910 nm. These blue GFP photons are indistinguishable from free NAD(P)H by both emission spectra and fluorescence lifetime. Therefore, NAD(P)H-FLIM in GFP-expressing cells will lead to incorrect interpretations of metabolic rates, and thus, these techniques should not be combined.

1. Introduction

Use of label-free imaging techniques are rapidly increasing, with many advantages in both clinical applications and basic research [1–3]. These imaging strategies typically exploit endogenous tissue properties (e.g. autofluorescence) to circumvent the need for genetically encoded indicators or organic dyes. One such method is fluorescence lifetime imaging (FLIM) of endogenous nicotinamide adenine dinucleotide (NADH) to monitor cellular metabolic changes. This is typically achieved by time-correlated single photon counting (TCSPC), using 2-photon laser scanning microscopy (2PLSM) of NADH autofluorescence, whose lifetime depends on intermolecular binding states (Fig. 1). In glycolysis, oxidized, non-fluorescent NAD^+ becomes reduced to fluorescent NADH. In this free, unbound state, NADH emits photons with a short fluorescence lifetime of 400 ps. However, upon enzymatic binding, such as to complex I of the electron transport chain (ETC), NADH is stabilized and its fluorescent lifetime increases to approximately 2000 ps, with reports ranging from 1000 – 5000 ps depending on binding partner [4–9] (Fig. 1(d), (e)). It is therefore possible to distinguish free and bound forms of NADH, and to extrapolate the ratio of glycolysis to ETC metabolism. As NADH is experimentally indistinguishable from the closely related nicotinamide adenine dinucleotide phosphate (NADPH) molecule by excitation and emission spectra or fluorescence lifetimes (though possible to computationally separate *post hoc* [8]), we refer to them jointly as NAD(P)H. NAD(P)H-FLIM has gleaned important roles of cellular metabolism in stem cell differentiation, cancer cell metastasis, and immune activation [9–13].

#359693 https://doi.org/10.1364/BOE.10.004381
Journal © 2019 Received 6 Feb 2019; revised 10 May 2019; accepted 17 May 2019; published 2 Aug 2019

Biomedical Optics EXPRESS

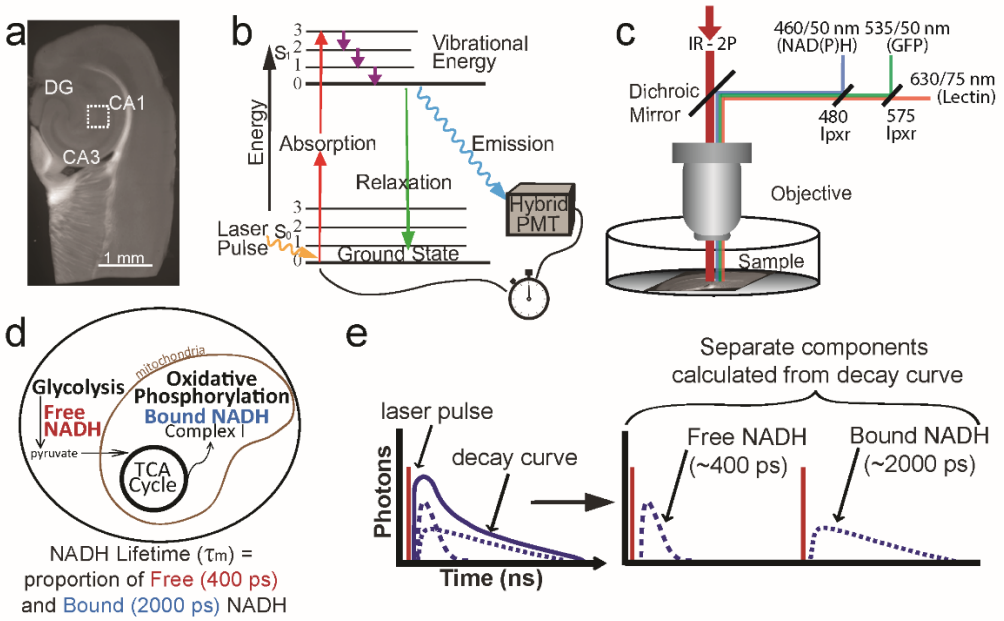

Fig. 1. NAD(P)H-FLIM. (a) Experiments were performed in the CA1 region of acute hippocampal slices. (b) A two-photon laser excites electrons of fluorescent molecules. Upon electron decay to ground state, a photon is released and detected by the hybrid PMT. The time of photon arrival is compared to the time of initial laser pulse, and the lifetime of the excited electron is calculated. (c) On a two-photon microscope, emitted light is passed through a series of long-pass dichroic mirrors and filter sets for NAD(P)H (460/50 nm), GFP (535/50 nm), or tomato lectin 594-DyLight (630/75 nm). (d) Endogenous NADH is autofluorescent and has a short lifetime of 400 ps when free, which increases to 2000 ps when enzymatically bound. (e) Based on photon arrival times, a biexponential curve (solid blue line) is fit to the data to separate photons into free or bound NADH components (dotted lines).

NAD(P)H-FLIM is a label-free technique that allows investigation of metabolically active tissue, thereby making the method applicable to *in vivo* or *ex vivo* preparations, including human samples [9,12,14,15]. Imaging cell-specific NAD(P)H in heterogenous tissue, however, requires a fluorescent reporter tag due to the ubiquity of NAD(P)H across cell types. The most commonly used cell marker in biology is green fluorescent protein (GFP).

GFP itself has also been investigated as a useful FLIM tool to measure intracellular pH, with reports of its lifetime varying from 2000 ps at pH 4.5 to 3000 ps at pH 7.5 [16,17]. Additional studies have reported a mean GFP lifetime of 2500 ps [10,18,19]. This lifetime is longer than that observed for bound (~2000 ps) or free (~400 ps) NAD(P)H, and the reported GFP emission is also spectrally separated from the blue NAD(P)H emission (510 nm vs 460 nm, respectively). Therefore, it stands to reason that these two fluorophores would be compatible to investigate cell-specific metabolism.

In this study, we examined the feasibility of using NAD(P)H-FLIM in brain tissue to measure metabolic states of cells identified by GFP expression. While GFP is well-known to fluoresce within the green spectrum with a peak at 510 nm, there are concerns based on early accounts of weaker emission in the blue spectrum (<460 nm) [20–22]. To our knowledge, there have been few reports describing the emission wavelength and lifetimes of this non-canonical blue GFP fluorescence. One such study used 2PLSM with 800 nm excitation to measure GFP emission properties in aqueous solution. They found green emission (514 nm) was well fit by a single exponential decay curve with a lifetime of 3000 ps, as expected and described by others. However, blue emission (456 nm) was better suited to a biexponential decay with a short (200 ps) lifetime component [19]. An additional study in cell culture found

Biomedical Optics EXPRESS

that GFP excitation at 740 nm exhibited blue emission at 450 nm with a triple exponential decay of τ_1: 110 ps, τ_2: 430 ps and τ_3: 2610 ps [18].

Although these studies describe the presence of blue GFP emission with short lifetimes, the impact on NAD(P)H-FLIM has not been examined. Pairing GFP identification with NAD(P)H-FLIM would be a powerful technique to measure the metabolic profile of specific cell types within their native, heterogeneous environments. However, the lesser-known blue fluorescence of GFP appears to match the emission spectrum and potentially the fluorescence lifetime of free NAD(P)H. We therefore sought to determine whether blue GFP photons would obscure NAD(P)H-FLIM measurements in GFP-positive cells.

We demonstrate that cellular expression of GFP leads to nearly complete contamination of the NAD(P)H signal. Using recombinant GFP in a sealed pipette, as well as neuronal and microglial expression of EGFP, we identify GFP emission in the blue spectrum (460 nm) with a mean lifetime around 500 ps when excited by NAD(P)H-FLIM parameters. Therefore, GFP expression would lead to the erroneous conclusion that cells are glycolytic, which highlights the necessity of ensuring appropriate cell-specific indicators are used in combination with NAD(P)H-FLIM.

2. Materials and methods

2.1 Animal protocols

All housing and experimental procedures were carried out in accordance with Canadian Council on Animal Care (CCAC) regulations. Wild type C57Bl/6 (WT), CX3CR1$^{+/EGFP}$ (Jackson Lab strain 005582 crossed with wild type C57Bl/6), or Thy1-EGFP mice (Jackson Lab strain 007788) on a C57Bl/6 background were housed on a 12 h light/day cycle with food and water *ad libitum*.

2.2 Acute hippocampal slice preparation

Adult mice (2 months of age) were anesthetized to surgical plane with isoflurane and decapitated according to protocols approved by the University of British Columbia committee on animal care. Brains were dissected and sliced horizontally with a vibratome (Leica VT1200S; Fig. 1(a)) at 300 µm thick in ice-cold NMDG slicing solution containing (in mM): 120 N-methyl-D-glucamine, 2.5 KCl, 25 $NaHCO_3$, 1 $CaCl_2$, 7 $MgCl_2$, 1.2 NaH_2PO_4, 20 D-glucose, 2.4 sodium pyruvate, and 1.3 sodium L-ascorbate, which was constantly oxygenated with 95% O_2 and 5% CO_2. Hippocampal slices were immediately transferred to artificial cerebral spinal fluid (aCSF) continuously oxygenated with 95% O_2 and 5% CO_2, and allowed to recover for 30 minutes at 32 °C. Artificial CSF contained (in mM): 126 NaCl, 2.5 KCl, 26 $NaHCO_3$, 2 $CaCl_2$, 2 $MgCl_2$, 1.25 NaH_2PO_4, and 10 D-glucose, pH 7.3–7.4, osmolarity 300 mOsm. For tomato lectin identification of microglia, slices were incubated with tomato lectin-594 DyLight (8 µg/ml; Vector Labs DL-1177) for 45 min at 32 °C.

2.3 Recombinant GFP

Recombinant GFP (EMD Millipore 14-392; 35 µM), was loaded into a glass micropipette (outer diameter: 1.5 mm; inner diameter 0.86 mm, sealed at one end with a microforge). The pipette was secured into a manipulator (Luigs & Neumann), and lowered into water for imaging by a water-immersion lens.

2.4 Imaging parameters

Hippocampal slices and recombinant GFP were imaged with a Coherent Chameleon Ultra II laser (mode-locked pulse train at 80 MHz) with a Zeiss LSM 7 MP microscope and Zeiss 20x-W/1.0 NA objective. Green and red fluorescence emission were detected by GaAsP photo-multiplier tubes (PMT; Zeiss LSM BiG), while blue NAD(P)H fluorescence lifetime

Biomedical Optics EXPRESS

emission was detected by a GaAsP hybrid detector (HPM-100-40 hybrid PMT, Becker and Hickl).

To image NAD(P)H lifetime in GFP-expressing cells, tissue was excited at 750 nm, and emitted light was split using a 480 nm long pass dichroic mirror. Blue NAD(P)H fluorescence passed through a 460/50 nm filter, while longer wavelengths were again split by a 575 nm long pass dichroic mirror (Chroma tech, Bellows Falls, VT). Green fluorescence was collected after passing through a 535/50 nm filter, while red (non-NAD(P)H autofluorescence or tomato lectin) passed through a 630/75 nm filter before detection (Chroma tech, Bellows Falls, VT; Fig. 1(c)). Images were taken in the stratum radiatum of CA1 hippocampus at a depth of 50 µm – 80 µm below the surface of the brain slice.

Recombinant GFP was imaged from 700 to 950 nm excitation, and emission was detected with the TCSPC hybrid-PMT using either an NAD(P)H filter (460/50 nm) for blue emission, or GFP filter (535/50 nm) for green emission. Images were acquired at 256 x 256 (zoom factor 2.8) over 30 seconds to ensure a sufficient number of photons were collected for curve fitting. For cross section measurements of recombinant GFP, laser excitation intensity was adjusted to achieve a consistent power output of 12.5 mW for green emission and 15 mW for blue emission (measured below the objective). Photons were collected for one minute in both cases for lifetime decay curve calculations. Note that it was necessary to use different excitation powers (15 mW for blue emission, and 12.5 mW for green emission) as the blue emission is dimmer across all excitation wavelengths, therefore normalized intensities are not directly comparable.

2.5 NAD(P)H fluorescence lifetime data

NAD(P)H photons collected by the hybrid-PMT were detected by a TCSPC module (SPC-150, Becker and Hickl, Berlin, Germany) and SPCM software (Becker and Hickl, Berlin, Germany). Laser pulse clock information was simultaneously sent to the SPC-150 module enabling lifetime calculations.

Photon counts were passed to SPC Image (version 7.3), where decay curves for each pixel were calculated using a two-component exponential by the following equation:

$$F(t) = \alpha_1 e^{-t/\tau_1} + \alpha_2 e^{-t/\tau_2} \quad (1)$$

Where α is the amplitude and τ is the lifetime. We processed the data with unfixed τ_1 and τ_2 lifetimes, which correspond to the free and bound forms of NAD(P)H, respectively (Fig. 1(d), e). The instrument response function (IRF) was automatically calculated by taking the derivative of the rising edge of the fluorescence signal. SPC Image performed automatic convolution of the decay model with this calculated IRF to best fit the measured data. There was no evidence of continued NAD(P)H emission past the 12 ns acquisition window set by the laser pulse rate, with only background photons detected at the onset of the following acquisition.

The mean lifetime (τ_m) of each pixel is calculated by:

$$\tau_m = \alpha_1 \tau_1 + \alpha_2 \tau_2 \quad (2)$$

where $\alpha_1 + \alpha_2 = 1$. The average mean lifetime across the image or mask of a cell was reported. A spatial bin factor with a radius of 3 pixels was used to attain a photon count >10 at the tail of the curve. Fluorescence lifetime of GFP was calculated as either a one or two-component decay curve, and the τ_m was recorded.

2.6 Single-cell NAD(P)H lifetime analysis

To measure NAD(P)H lifetime within single cells, a mask was drawn around the cell using either the EGFP or tomato lectin fluorescence image as a guide. Masks were drawn away from the edge of the cell to avoid any pixels contaminated by photons from the surrounding

Biomedical Optics EXPRESS

tissue. The τ_m of the mask was recorded. Results were compared by a Student's t-test or one-way ANOVA as specified, and reported or displayed as mean ± SD.

3. Results

3.1 Recombinant GFP lifetime under NAD(P)H imaging parameters

GFP is reported to have a mean lifetime of 2500 ps [10,18]. However, this is measured using excitation and emission wavelengths ideal for imaging GFP (2P λ_{ex}: 910 nm, λ_{em}: 510 nm). To test if the presence of GFP interferes with metabolic recordings, we measured GFP emission in the blue spectrum using NAD(P)H imaging parameters (2P λ_{ex}: 750 nm, λ_{em} filter: 460/50 nm). To accomplish this, the fluorescence lifetime of recombinant GFP (35 µM) was measured in a sealed micropipette to circumvent potential contamination from NAD(P)H, cellular components, and pH changes. The concentration and environment of GFP remained constant while the excitation and emission settings could be adjusted. When imaged at λ_{ex} 910 nm with 2PSLM, GFP is expected to fluoresce from 470 nm to 650 nm, with a peak at 510 nm [23]. To test the lifetime of both green and blue emission in these excitation parameters, emitted photons were collected by the TCSPC detector using either a green (535/50 nm) or blue (460/50 nm) emission filter. The mean lifetime measured through both emission filters approximated 2500 ps (Fig. 2(a), (b)). The histograms of each image show a well-defined peak, and both τ_1 and τ_2 are approximately 2500 ps with an equal split between the contributions of the components (α_1 and α_2), suggesting these data would fit to a single-component decay curve. The data were processed as a bi-exponential decay curve to match the parameters used for NAD(P)H lifetime calculations. These values correlate well with the previously measured lifetime of GFP [16,17].

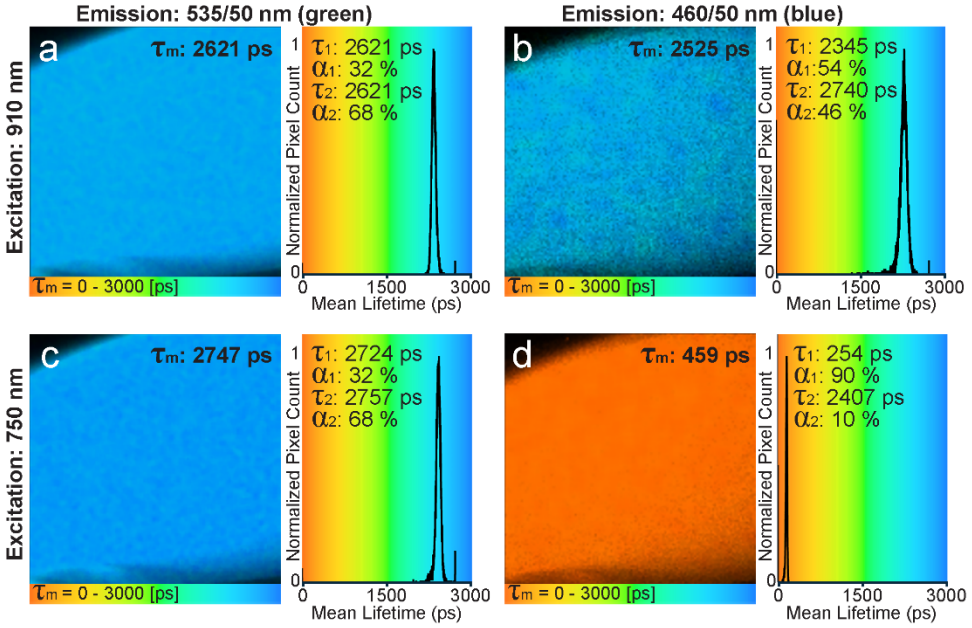

Fig. 2. Recombinant GFP lifetime across excitation and emission settings. Recombinant GFP protein in a sealed pipette was imaged with 910 nm or 750 nm excitation wavelengths. Either a green (535/50 nm) or blue (460/50 nm) emission filter was used before collecting light with the FLIM hybrid detector. Mean GFP lifetimes are over 2500 ps using 910 nm excitation with either the green (a), or the blue emission filter (b). Mean lifetime is also over 2500 ps using 750 nm excitation and the green emission filter (c). Using 750 nm excitation and the blue emission filter, the mean lifetime of GFP is 459 ps (d). Distribution of lifetimes are plotted as histograms showing the normalized number of pixels across mean lifetimes.

Biomedical Optics EXPRESS

GFP lifetime was then measured using 750 nm excitation to mimic NAD(P)H imaging conditions. Green emission once again exhibited an expected mean lifetime of 2500 ps (Fig. 2(c)). However, the blue emission had a short mean lifetime (τ_m ~500 ps) closely matching that of free NAD(P)H (Fig. 2(d)). These data confirm that, in the absence of NAD(P)H autofluorescence, GFP itself emits blue light with a short lifetime that is detectable with 750 nm, but not 910 nm, excitation.

To further characterize the blue and green GFP lifetimes and intensities, we measured these parameters using recombinant GFP across an excitation spectrum of 700 – 950 nm. Blue emission had a short mean lifetime from 700 to 800 nm due to a predominant τ_1 component (τ_m ~500 ps, α_1: 83-87%; lifetimes fixed at τ_1: 267 ps, τ_2: 2330 ps based on the average lifetimes from 700 to 800 nm excitation; Fig. 3(a)). At excitation wavelengths over 800 nm, there is a precipitous increase in mean lifetime to 2500 ps. The normalized emission intensity (Fig. 3(b)) reveals fewer photons are emitted at lower wavelengths relative to the peak intensity around 900 nm. As expected, the green emission showed a long and stable mean lifetime around 2500 ps (Fig. 3(c)), and an emission intensity increasing at longer wavelengths with a shoulder at 800 nm (Fig. 2(d)).

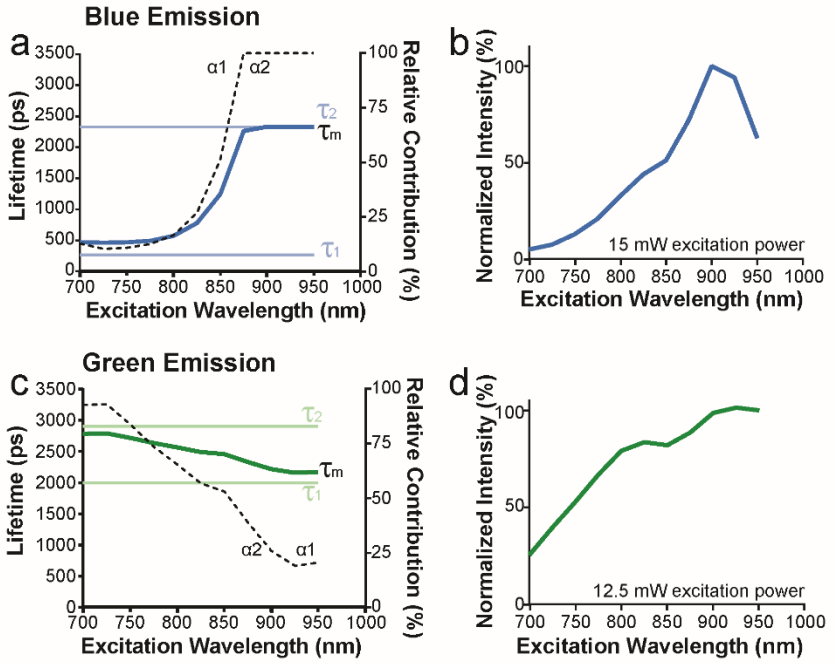

Fig. 3. Recombinant GFP emission lifetime and intensity spectra. Recombinant GFP protein in a sealed pipette was imaged from 700 nm to 950 nm excitation wavelengths at intervals of 25 nm. Either a blue (460/50 nm) or green (535/50 nm) emission filter was used before collecting light with the FLIM hybrid detector. Mean GFP lifetimes (τ_m; bold line) and the corresponding short (τ_1) and long (τ_2) lifetimes are shown across excitation lifetimes for blue (a) and green (c) emission. τ_1 and τ_2 lifetimes were fixed based on the average unfixed values from 700 – 825 nm. The relative contribution of the short (α_1) and long (α_2) lifetimes are represented as percentage of the total photons (dashed line). Intensities of blue (b) and green (d) GFP emission were measured across excitation wavelengths as the number of photons collected and normalized to the peak emission intensity.

3.2 NAD(P)H measurements in Thy1-EGFP neurons

To investigate the GFP contamination of NAD(P)H fluorescence in a biological system, we turned to Thy1-EGFP mice that express EGFP in a subset of neurons. As an important control, we evaluated the metabolic profile of wild type (WT; non-EGFP) pyramidal neurons

Biomedical Optics EXPRESS

in the CA1 region of WT hippocampus. Neurons were identified with transmitted light (Fig. 4(a)) and NAD(P)H-FLIM was imaged using 2PLSM tuned to 750 nm. We observed perinuclear NAD(P)H fluorescence with a heterogeneous distribution of lifetimes denoting the abundance of free (glycolytic) and bound (ETC) NAD(P)H, with an average mean lifetime of 1193 ± 44 ps across cells (τ_1: 550 ps, α_1: 70%; τ_2: 2500 ps, α_2: 30%; Fig. 4(b)).

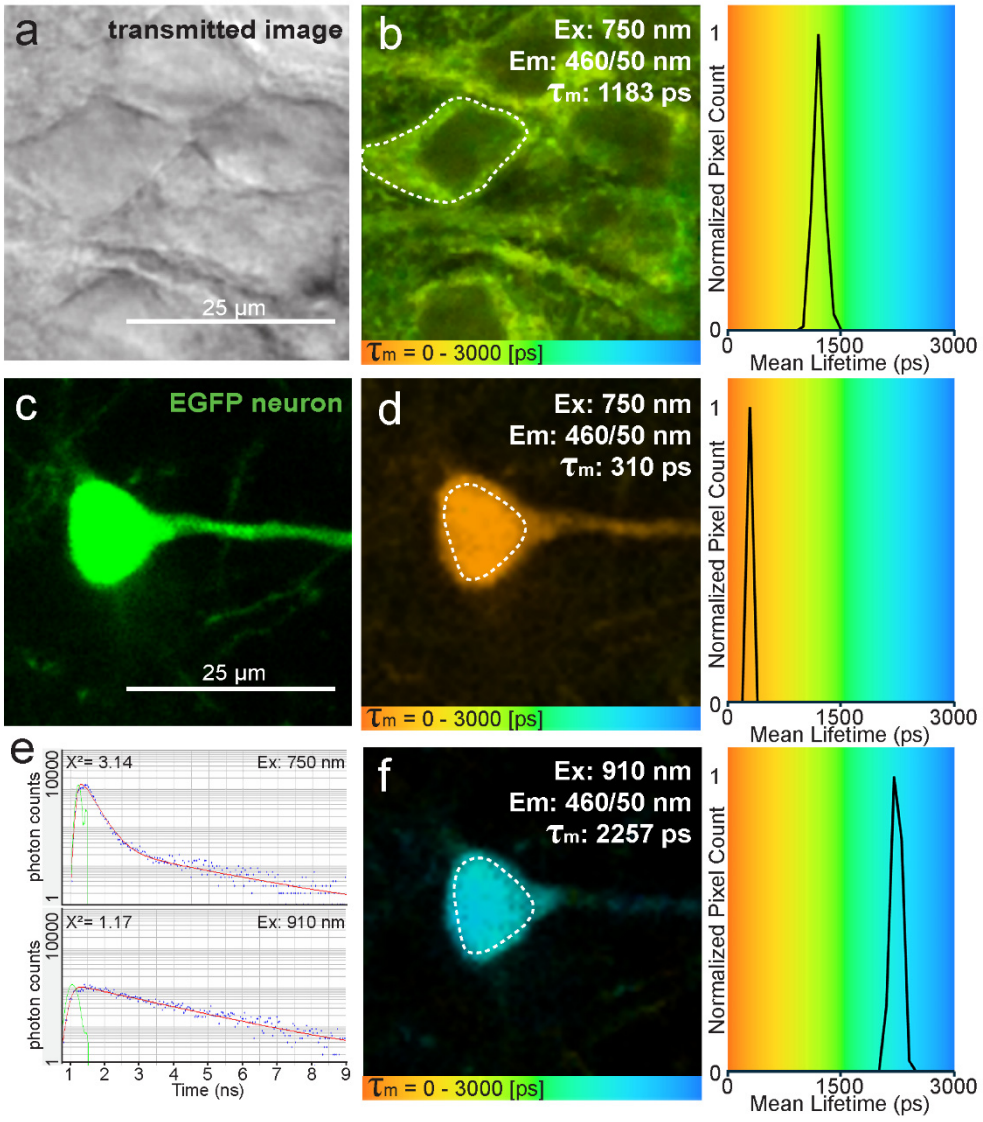

Fig. 4. NAD(P)H measurements of Thy1-EGFP neurons *in situ*. (a) Non-EGFP neurons are identified by transmitted light. (b) NAD(P)H mean lifetime is 1183 ps, representing a mix of bound and free NAD(P)H species. Thy1-EGFP neurons (c) were imaged with either 750 nm (d) or 910 nm (f) excitation, using the NAD(P)H (460/50 nm) emission filter. Distribution of lifetimes are plotted as histograms showing the normalized number of pixels across mean lifetimes. Only pixels within the neuron mask (dotted line in b, d, and f) are considered. (e) Decay curves within traced mask generated with 750 nm (top) or 910 nm (bottom) excitation.

In contrast, performing NAD(P)H-FLIM in Thy1-EGFP neurons (Fig. 4(c)) revealed a short mean lifetime (τ_m: 290 ± 25 ps; τ_1: 280 ps, α_1: 98%; τ_2: 2400 ps, α_2: 2%), incorrectly suggesting a high rate of glycolysis over ETC (Fig. 4(d), (e) top). As confirmation of the

Biomedical Optics EXPRESS

EGFP lifetime in these conditions, excitation of Thy1-EGFP neurons at 910 nm produced the expected EGFP lifetime near 2500 ps (τ_1: 2000 ps, α_1: 80%, τ_2: 2500 ps, α_2: 20%; Fig. 4(e) bottom, (f)). As the blue emission of GFP decreases at lower excitation wavelengths (Fig. 3(b)), EGFP-expressing neurons were imaged at 710 nm, 725 nm, and 750 nm excitation. The short EGFP component was observed in all conditions, suggesting EGFP and NAD(P)H cannot be differentiated at shorter excitation wavelengths. Therefore, we have confirmed that the lifetime of EGFP in the blue emission spectrum mimics that of free NAD(P)H in biological tissue, and in this case, overwhelms the endogenous NAD(P)H signal and cannot be confidently separated by experimental conditions.

3.3 Cell-specific metabolism in EGFP-negative systems

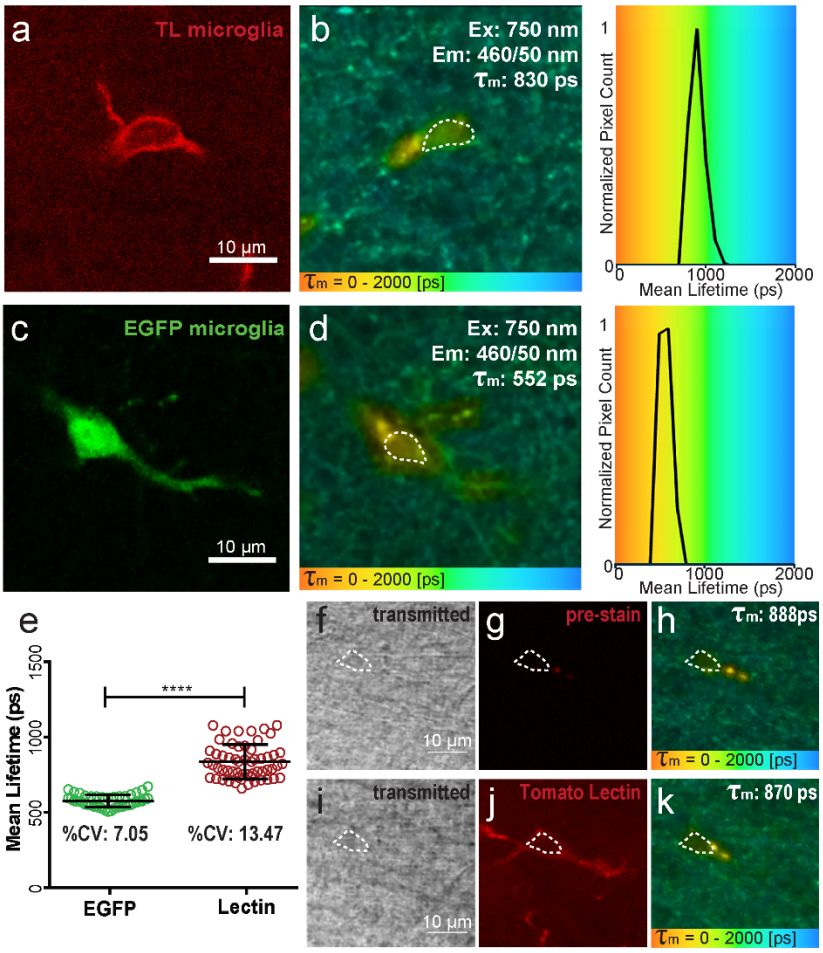

Fig. 5. EGFP-expressing microglia have shorter NAD(P)H mean lifetimes. Wild type microglia identified by tomato lectin 594-DyLight (a), and corresponding NAD(P)H lifetime measurement (b). EGFP-expressing microglia imaged at 750 nm excitation with a 535/50 nm filter (c), or 460/50 nm filter to collect NAD(P)H emission (d). Distribution of lifetimes are plotted as histograms showing the normalized number of pixels across mean lifetimes. Only pixels within microglia cell masks (dotted line in b and d) are considered. (e) Comparison of mean NAD(P)H lifetime and coefficients of variation (%CV) from microglia with or without EGFP expression. Microglia were identified by transmitted light and imaged before (f,g,h), and after (i,j,k) tomato lectin application. **** $p < 0.0001$ by Student's t-test; error bars show standard deviation of the mean.

Biomedical Optics EXPRESS

As an alternative to EGFP expression, exogenous dyes may be used as cell-specific indicators. To test the impact of a red-shifted, externally-applied dye on the NAD(P)H-FLIM signal, we turned to microglia in acute hippocampal slices. It has been previously established that these cells can be identified by incubation with Isolectin-B4, or tomato lectin, which binds to the extracellular surface with no adverse effect on their physiology [24–26]. To image EGFP-negative microglia, WT C57Bl/6 acute hippocampal slices were incubated with tomato lectin-594 DyLight (8 µg/ml; Vector Labs DL-1177) for 45 min at 32 °C as previously described [24]. In microglia identified by this method, the NAD(P)H mean lifetime was 837 ps (SD: ± 113 ps) (Fig. 5(a), (b)).

As confirmation that tomato lectin staining does not directly interfere with NAD(P)H-FLIM measurements or change microglial metabolism, microglia were imaged before and after tomato lectin application. Microglia were initially identified by transmitted light and lipofuscin autofluorescent inclusions to measure NAD(P)H lifetime (Fig. 5(f), (g), (h)). Tomato lectin was then puffed onto the slice to stain microglia, and the NAD(P)H lifetime was again measured (Fig. 5(i), (j), (k)). Pre- and post-lectin images showed no difference in NAD(P)H mean lifetime (τ_m: 912 ± 50 ps pre-tomato lectin; τ_m: 889 ± 50 ps post-tomato lectin, n.s. by one-way ANOVA including EGFP and tomato-lectin incubation tissue). Therefore, tomato lectin staining is a reliable way to identify microglia in heterogeneous *ex vivo* conditions without effecting cell metabolism or NAD(P)H-FLIM measurements.

3.4 NAD(P)H measurements in CX3CR1-EGFP microglia

To confirm the effect of EGFP on the NAD(P)H signal within microglia, acute hippocampal slices from CX3CR1$^{+/EGFP}$ mice were imaged. Comparing the NAD(P)H lifetime of several microglia by EGFP expression or tomato lectin staining revealed that EGFP-positive microglia have significantly shorter mean lifetimes (τ_m: 577 ± 41 ps in EGFP-positive cells, Fig. 5(c), (d); τ_m: 837 ± 113 ps in EGFP-negative cells), further confirming the bright EGFP emission in the blue spectrum with a short fluorescent lifetime. Microglia identified by tomato lectin also have a larger standard deviation around the mean relative to EGFP-positive cells (coefficient of variation: EGFP 7.05%; tomato lectin 13.47%; Fig. 5(e)) denoting complex metabolic pathways. This provides further evidence that EGFP expression overwhelms NAD(P)H signals within biological systems.

3.5 Reactive oxygen species and protein load on NAD(P)H measurements

While we confirm that recombinant EGFP fluoresces in the blue spectrum with a lifetime around 500 ps in biological systems, it is possible that the altered NAD(P)H-FLIM measurements in EGFP-positive cells is the result of a metabolic alteration caused by EGFP protein expression. Responses to EGFP expression might include reactive oxygen species (ROS) load [27], or cell and ER stress induced by exogenous protein expression [28]. To address the concern of increased ROS in EGFP-expressing cells, CX3CR1$^{+/EGFP}$ slices were incubated with the ROS scavengers N-acetyl-cysteine (5 mM) and ascorbic acid (2 mM). Addition of these ROS buffers did not rescue the NAD(P)H measurements of EGFP-positive microglia to tomato lectin levels (τ_m: 619 ± 68 ps in ROS scavenger incubated EGFP microglia; Fig. 6).

Biomedical Optics EXPRESS

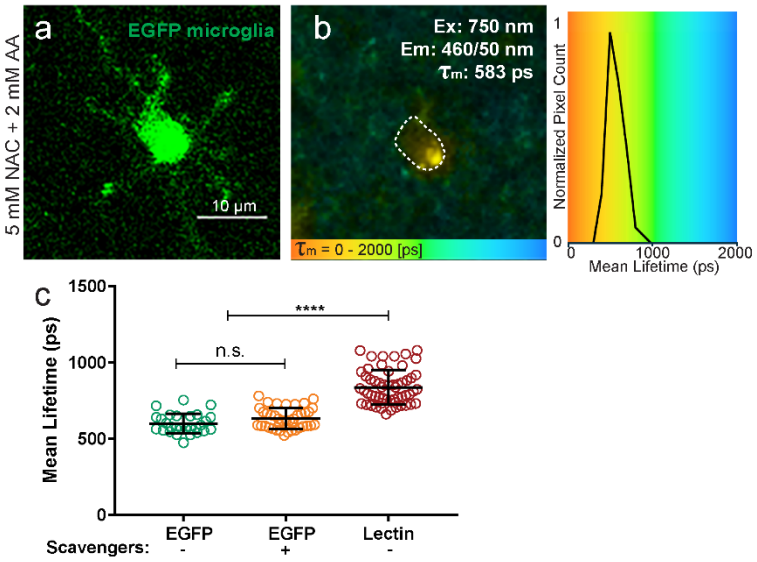

Fig. 6. ROS scavengers do not increase NAD(P)H lifetimes in EGFP expressing microglia. Acute hippocampal slices with EGFP-positive microglia were incubated for 1 hour in 5 mM N-acetyl cysteine and 2 mM ascorbic acid before imaging (a). Microglial NAD(P)H lifetime in the presence of ROS scavengers was ~583 ps. Distribution of lifetimes are plotted as a histogram showing the normalized number of pixels across mean lifetimes. Only pixels within the microglia cell mask (dotted line) are considered (b). (c) ROS scavengers did not significantly increase the mean lifetimes of EGFP-positive microglia, which were still significantly shorter than microglia from wild type slices identified by lectin (same lectin data set as presented in Fig. 5(e)). **** $p < 0.0001$ by one-way ANOVA; error bars show standard deviation of the mean.

To investigate the role of exogenous protein expression and associated cellular and ER stress, NAD(P)H-FLIM was performed on the CX3CR1-Cre mouse line. In these mice, microglia express the Cre protein under the same promoter as used to drive EGFP in the $CX3CR1^{+/EGFP}$ line. Therefore, if metabolic changes resulted from exogenous protein expression, these cells should also display a short NAD(P)H lifetime as seen in EGFP-positive tissue. However, all Cre-expressing microglia showed a similar NAD(P)H measurement to those from WT cells (Cre-microglia τ_m: 998 ps; Fig. 7). As in WT microglia (Fig. 5(a), (b), (e)), Cre-expressing microglia have a significantly longer mean lifetime, with a greater coefficient of variation when compared to EGFP-positive cells (τ_m: 573 ± 42 ps in EGFP cells; τ_m: 1067 ± 197 ps in Cre cells; Fig. 7(c)).

Biomedical Optics EXPRESS

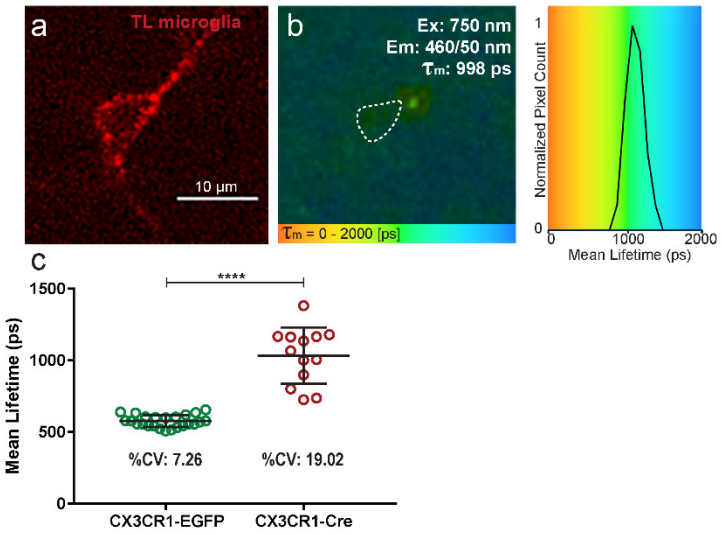

Fig. 7. Exogenous protein expression does not cause short NAD(P)H lifetime measurements. Microglia were identified by tomato lectin staining in acute hippocampal slices from mice expressing a Cre protein under the CX3CR1 promoter (a). The NAD(P)H lifetime in these cells was 998 ps (b). Distribution of lifetimes are plotted as a histogram showing the normalized number of pixels across mean lifetimes. Only pixels within the microglia cell mask (dotted line) are considered. (c) NAD(P)H lifetimes in Cre-expressing microglia are significantly higher and with a larger coefficient of variation than from EGFP-positive cells. **** $p < 0.0001$ by Student's t-test; error bars show standard deviation of the mean.

4. Discussion

We have tested the possibility that combining NAD(P)H-FLIM with EGFP expression could be used to measure cell-type specific metabolism within heterogeneous tissue preparations. NAD(P)H-FLIM is an effective imaging technique to quantify shifts in metabolic states. However, we show here that despite the spectral separation of reported NAD(P)H and EGFP emissions, exciting either GFP or EGFP at 750 nm yields blue emission at 460 nm that contaminates NAD(P)H fluorescence. This was confirmed both in aqueous solution and *ex vivo* in neurons and microglia. All EGFP-positive cells imaged with NAD(P)H-FLIM parameters possessed an artifactual glycolytic phenotype due to EGFP molecules fluorescing in the blue spectrum with a short lifetime matching free NAD(P)H.

The EGFP and free NAD(P)H components could not be confidently separated using different excitation wavelengths. Further, EGFP expression masked metabolic changes to NAD(P)H as 10 min exposure to hypoxia had no effect on emission lifetime in the blue spectrum (data not shown). EGFP separation was also attempted by using a three component model to fit the decay curve with fixed τ_2 and τ_3 at the expected free and bound NAD(P)H lifetimes, respectively. While this method uncovers an additional short component with a lifetime matching the τ_1 of recombinant GFP, it is still unclear if EGFP photons are contributing to the fixed free NAD(P)H component. Based on our experience, this method does not reliably separate the EGFP photons and it is not recommended without further validation. The contribution of EGFP and NAD(P)H may change across cell types, expression patterns, or experimental setups, and may therefore be separable under certain conditions. However, the presence of EGFP will nevertheless introduce noise and decrease the dynamic range of the NAD(P)H signal, and in so doing, decrease confidence in the resulting data. It is instead suggested that EGFP-expressing tissue is avoided when performing NAD(P)H-FLIM measurements.

Biomedical Optics EXPRESS

In practice, endogenous NAD(P)H autofluorescence has low emission intensity, while EGFP is bright and often expressed at high levels. Furthering the problem is the unexpectedly high quantum yield of GFP in the blue spectrum after 2PLSM relative to one-photon excitation [19]. Therefore, EGFP contamination of the blue channel is likely to completely obscure the NAD(P)H signal in common experimental preparations. NAD(P)H-FLIM measurements in GFP-expressing cells have been performed previously to investigate macrophage metabolism or metabolic effects of viral infection [29,30]. A high rate of glycolysis and low ETC activity in GFP-positive cells was reported [30]. Indeed, their measurements have little deviation around the mean and are centred at 500 ps, which is what we have observed to be the GFP lifetime under NAD(P)H imaging conditions. Without GFP-negative experiments, the results are difficult to interpret, which underscores the importance of appropriate controls when using FLIM techniques in combination with fluorescent proteins and dyes.

It is well established that the GFP chromophore exists in both anionic deprotonated (R^-), and neutral protonated (RH) states [21,31]. The deprotonated form is structurally relaxed and emits at a peak around 510 nm with a monoexponential decay curve and lifetime of 3200 ps [20]. However, when protonated, the GFP excitation peak is shifted to ~395 nm from the typical peak at ~475 nm. The protonated form first undergoes excited state proton transfer to a structurally unstable intermediate form, which shows emission at 510 nm, but also a unique blue fluorescence [20–22]. To investigate the lifetime of this blue fluorescence, prior studies have used a GFP mutant (T203V) with an increased fraction of protonated protein. Researchers found that fitting a lifetime curve at 515 nm emission revealed a lifetime around 3290 ps. However, fitting the lifetime curve at 460 nm revealed a tri-component decay curve, τ_1 of 70 ps (68%) which falls within the instrument response function, τ_2 of 420 ps (25%), and τ_3 of 1210 ps (7%) [20]. The observation of blue emission with short fluorescence lifetime has also been confirmed using 2P excitation at 740 nm [18]. Therefore, our work agrees with previously published results that a subset of protonated GFP molecules can emit in the blue spectra with a short fluorescence lifetime. This also reconciles the absence of a short lifetime emission when GFP is imaged at 910 nm, as this is less likely to excite the protonated chromophore.

We explored several other possible mechanisms which could lead to the observed GFP effect in NAD(P)H-FLIM recordings. These include biological effects of GFP expression on cellular metabolism such as ROS production, or protein load and cell stress.

It has been previously reported that the maturation of each GFP molecule releases a hydrogen peroxide molecule [27]. While it is speculated that the originating jellyfish species, *Aequorea Victoria,* have evolved ROS scavenging mechanisms to cope with increased oxidative stress, artificial expression in mammalian cells may cause stress and damage. Furthermore, this altered redox state may impair the function of complexes within the ETC and force the cell to rely on glycolysis for energy production [32]. While this should remain a consideration to the health and understanding of biological experiments, it does not appear to be the cause of the short lifetime signal in our NAD(P)H-FLIM experiments. Addition of ROS scavengers (N-acetyl-cysteine, and ascorbic acid) did not alter the NAD(P)H signal within EGFP-positive microglia (Fig. 6). We cannot, however, experimentally rule-out possible chronic ROS-induced changes to the cytosolic milieu that are not amenable to transient ROS scavenging.

The short lifetime signal in EGFP-positive cells also does not appear to be the result of exogenous protein expression and associated cellular stress [28], as we did not observe a ‘glycolytic’ shift in lifetimes from CX3CR1-Cre tissue (Fig. 7). The absence of a Cre-dependent shift in NAD(P)H lifetimes compared to control cells points toward a technical artifact from EGFP fluorescence, rather than a metabolic effect of EGFP on biological tissue. The clearest example of this is shown in imaging recombinant GFP solution within a

Biomedical Optics EXPRESS

micropipette (Fig. 2 and 3), where there is no confounding effect of metabolic changes or variable cytoplasmic conditions.

While researchers should be aware of these unintended consequences of using genetically encoded indicators, we provide evidence that the EGFP effect on NAD(P)H-FLIM measurements is a result of emission in the blue spectrum with a short lifetime.

5. Conclusion

In conclusion, we have shown that when either GFP or EGFP are excited at 750 nm, there is a strong emission in the blue spectrum (~460 nm) with a short mean lifetime (~500 ps). This is likely due to excitation and detection of a fraction of GFP molecules in the protonated form. As these are the same imaging parameters used to measure NAD(P)H lifetime, the use of EGFP-expressing cells will lead to incorrect interpretations of cellular metabolism. Instead, to perform cell-specific metabolic measurements, we encourage investigators to use fluorophores with no emission in the blue spectrum. We remind researchers of the importance of testing their fluorescent molecules under NAD(P)H imaging conditions to ensure they are reliably measuring only NAD(P)H metabolism.

Funding

Canadian Institutes of Health Research (CIHR); Fondation Leducq; Michael Smith Foundation for Health Research.

Acknowledgments

Canadian Institutes of Health Research (CIHR) Canada Research Chair (CRC) in Neuroscience to B.A.M., a Foundation Grant (148397); Fondation Leducq Grant to B.A.M.

E.M.Y. was additionally supported by a Canadian Institutes of Health Research (CIHR) Doctoral Scholarship, and a University of British Columbia 4-Year Fellowship.

N.L.W. holds Michael Smith Foundation for Health Research and CIHR Banting Fellowships.

Disclosures

The authors declare that there are no conflicts of interest related to this article.

References

1. M. Lombardo, D. Merino, P. Loza-Alvarez, and G. Lombardo, "Translational label-free nonlinear imaging biomarkers to classify the human corneal microstructure," Biomed. Opt. Express **6**(8), 2803–2818 (2015).
2. P. Büttner, R. Galli, D. Husser, and A. Bollmann, "Label-free imaging of myocardial remodeling in atrial fibrillation using nonlinear optical microscopy: A feasibility study," J. Atr. Fibrillation **10**(5), 1644 (2018).
3. Y. Jing, Y. Wang, X. Wang, C. Song, J. Ma, Y. Xie, Y. Fei, Q. Zhang, and L. Mi, "Label-free imaging and spectroscopy for early detection of cervical cancer," J. Biophotonics **11**(5), e201700245 (2018).
4. D. K. Bird, L. Yan, K. M. Vrotsos, K. W. Eliceiri, E. M. Vaughan, P. J. Keely, J. G. White, and N. Ramanujam, "Metabolic mapping of MCF10A human breast cells via multiphoton fluorescence lifetime imaging of the coenzyme NADH," Cancer Res. **65**(19), 8766–8773 (2005).
5. J. Vergen, C. Hecht, L. V Zholudeva, M. M. Marquardt, and M. G. Nichols, "Metabolic imaging using two-photon excited NADH intensity and fluorescence lifetime imaging," Microsc Microanal. **18**(4), 761 (2013).
6. J. R. Lakowicz, H. Szmacinski, K. Nowaczyk, and M. L. Johnson, "Fluorescence lifetime imaging of free and protein-bound NADH," Proc. Natl. Acad. Sci. U.S.A. **89**(4), 1271–1275 (1992).
7. H. Schneckenburger, M. Wagner, P. Weber, W. S. L. Strauss, and R. Sailer, "Autofluorescence lifetime imaging of cultivated cells using a UV picosecond laser diode," J. Fluoresc. **14**(5), 649–654 (2004).
8. T. S. Blacker, Z. F. Mann, J. E. Gale, M. Ziegler, A. J. Bain, G. Szabadkai, and M. R. Duchen, "Separating NADH and NADPH fluorescence in live cells and tissues using FLIM," Nat. Commun. **5**, 3936 (2014).
9. M. A. Yaseen, S. Sakadžić, W. Wu, W. Becker, K. A. Kasischke, and D. A. Boas, "In vivo imaging of cerebral energy metabolism with two-photon fluorescence lifetime microscopy of NADH," Biomed. Opt. Express **4**(2), 307–321 (2013).
10. C. Stringari, A. Cinquin, O. Cinquin, M. A. Digman, P. J. Donovan, and E. Gratton, "Phasor approach to fluorescence lifetime microscopy distinguishes different metabolic states of germ cells in a live tissue," Proc.

Biomedical Optics EXPRESS

Natl. Acad. Sci. U.S.A. **108**(33), 13582–13587 (2011).
11. C. Stringari, J. L. Nourse, L. A. Flanagan, and E. Gratton, "Phasor Fluorescence Lifetime Microscopy of Free and Protein-Bound NADH Reveals Neural Stem Cell Differentiation Potential," PLoS One **7**(11), e48014 (2012).
12. C. Stringari, H. Wang, M. Geyfman, V. Crosignani, V. Kumar, J. S. Takahashi, B. Andersen, and E. Gratton, "In Vivo Single-Cell Detection of Metabolic Oscillations in Stem Cells," Cell Reports **10**(1), 1–7 (2015).
13. A. Alfonso-García, T. D. Smith, R. Datta, T. U. Luu, E. Gratton, E. O. Potma, and W. F. Liu, "Label-free identification of macrophage phenotype by fluorescence lifetime imaging microscopy," J. Biomed. Opt. **21**(4), 046005 (2016).
14. M. C. Skala, K. M. Riching, D. K. Bird, A. Gendron-fitzpatrick, J. Eickhoff, K. W. Eliceiri, P. J. Keely, and N. Ramanujam, "In vivo Multiphoton Fluorescence Lifetime Imaging of Protein-bound and Free NADH in Normal and Pre-cancerous Epithelia," J. Biomed. Opt. **12**(2), 1–19 (2007).
15. D. Pouli, M. Balu, C. A. Alonzo, Z. Liu, K. P. Quinn, R. M. Harris, K. M. Kelly, and B. J. Tromberg, "Imaging mitochondrial dynamics in human skin reveals depth- dependent hypoxia and malignant potential for diagnosis," Sci. Transl. Med. **8**, 367ra169 (2017).
16. W. Li, K. D. Houston, and J. P. Houston, "Shifts in the fluorescence lifetime of EGFP during bacterial phagocytosis measured by phase-sensitive flow cytometry," Sci. Rep. **7**, 1–11 (2017).
17. T. Nakabayashi, H.-P. Wang, M. Kinjo, and N. Ohta, "Application of fluorescence lifetime imaging of enhanced green fluorescent protein to intracellular pH measurements," Photochem. Photobiol. Sci. **7**(6), 668–670 (2008).
18. S. T. Hess, E. D. Sheets, A. Wagenknecht-Wiesner, and A. A. Heikal, "Quantitative analysis of the fluorescence properties of intrinsically fluorescent proteins in living cells," Biophys. J. **85**(4), 2566–2580 (2003).
19. A. Volkmer, V. Subramaniam, D. J. Birch, and T. M. Jovin, "One- and two-photon excited fluorescence lifetimes and anisotropy decays of green fluorescent proteins," Biophys. J. **78**(3), 1589–1598 (2000).
20. G. Jung, J. Wiehler, and A. Zumbusch, "The photophysics of green fluorescent protein: influence of the key amino acids at positions 65, 203, and 222," Biophys. J. **88**(3), 1932–1947 (2005).
21. M. Chattoraj, B. A. King, G. U. Bublitz, and S. G. Boxer, "Ultra-fast excited state dynamics in green fluorescent protein: multiple states and proton transfer," Proc. Natl. Acad. Sci. U.S.A. **93**(16), 8362–8367 (1996).
22. O. Shimomura and F. H. Johnson, "Properties of the Bioluminescent Protein Aequorin," Biochemistry **8**(10), 3991–3997 (1969).
23. M. Chalfie, Y. Tu, G. Euskirchen, and W. W. Ward, "Green Fluorescent Protein as a Marker for Gene Expression," Science **263**(5148), 802–805 (1994).
24. B. Schwendele, B. Brawek, M. Hermes, and O. Garaschuk, "High-resolution in vivo imaging of microglia using a versatile nongenetically encoded marker," Eur. J. Immunol. **42**(8), 2193–2196 (2012).
25. F. Boscia, C. L. Esposito, A. Casamassa, V. de Franciscis, L. Annunziato, and L. Cerchia, "The isolectin IB4 binds RET receptor tyrosine kinase in microglia," J. Neurochem. **126**(4), 428–436 (2013).
26. W. J. Streit, "An Improved Staining Method for Rat Microglial Cells Using the Lectin from Griffonia simplicifolia," J. Histochem. Cytochem. **38**(11), 1683–1686 (1990).
27. D. Ganini, F. Leinisch, A. Kumar, J. Jiang, E. J. Tokar, C. C. Malone, R. M. Petrovich, and R. P. Mason, "Fluorescent proteins such as eGFP lead to catalytic oxidative stress in cells," Redox Biol. **12**(March), 462–468 (2017).
28. J. Mandl, T. Mészáros, G. Bánhegyi, and M. Csala, "Minireview: Endoplasmic Reticulum Stress: Control in Protein, Lipid, and Signal Homeostasis," Mol. Endocrinol. **27**(3), 384–393 (2013).
29. N. Mazumder, R. K. Lyn, R. Singaravelu, A. Ridsdale, D. J. Moffatt, C. W. Hu, H. R. Tsai, J. McLauchlan, A. Stolow, F. J. Kao, and J. P. Pezacki, "Fluorescence Lifetime Imaging of Alterations to Cellular Metabolism by Domain 2 of the Hepatitis C Virus Core Protein," PLoS One **8**(6), e66738 (2013).
30. J. M. Szulczewski, D. R. Inman, D. Entenberg, S. M. Ponik, J. Aguirre-Ghiso, J. Castracane, J. Condeelis, K. W. Eliceiri, and P. J. Keely, "In Vivo Visualization of Stromal Macrophages via label-free FLIM-based metabolite imaging," Sci. Rep. **6**(1), 25086 (2016).
31. H. L. A. Kummer, R. Heinecke, F. P. C. Kompa, G. Bieser, T. Jonsson, C. M. Silva, M. M. Yang, D. C. Youvan, and M. E. Michel-beyerle, "Time-resolved spectroscopy of wild-type and mutant Green Fluorescent Proteins reveals excited state deprotonation consistent with fluorophore-protein interactions," Chem. Phys. **213**, 1 (1996).
32. O. Marcillat, Y. Zhang, and K. J. Davies, "Oxidative and non-oxidative mechanisms in the inactivation of cardiac mitochondrial electron transport chain components by doxorubicin," Biochem. J. **259**(1), 181–189 (1989).